Feedback Linearization-Based Perimeter Controllers for Oversaturated Regions

©SHUTTERSTOCK.COM/HUNG CHUNG CHI

Digital Object Identifier 10.1109/MITS.2020.2970189
Date of current version: 23 March 2020

Qian Chen and Shihua Li*, *Fellow, IEEE*
Are with the School of Automation, Southeast University, and Key Laboratory of Measurement and Control of Complex Systems of Engineering, Ministry of Education, Nanjing 210096, China.
E-mail: cqcsaxyz@163.com; lsh@seu.edu.cn

Chengchuan An, Jingxin Xia, and Wenming Rao
Are with the School of Transportation, Southeast University, and the Intelligent Transportation System Research Center, Ministry of Education, Nanjing 210096, China.
E-mail: anchengchuan@seu.edu.cn; xiajingxin@seu.edu.cn; raowenming@seu.edu.cn

***Abstract*—**This paper concerns the perimeter control problem in the oversaturated region. The road network system is a nonlinear system. However, the existing achievements in the perimeter control setting are obtained by partially linearizing the system model around the point of interest, which is a local linearization and probably leads to lower traffic performances. To this end, a feedback linearization-based proportional and integral perimeter controller is developed to regulate the overall traffic state towards the desired accumulation state. Theoretical analysis demonstrates that the proposed feedback linearization-based control method can guarantee the exponentially asymptotic convergence of the protected road network state to the desired one. To evaluate the proposed methodology, extensive simulation tests are conducted, in which the proposed controller is compared with the existing proportional and integral control strategy. The results indicate that the proposed feedback linearization-based proportional and integral perimeter controller can: (i) relieve the overall congestion in the urban network; and (ii) enhance the traffic performance in terms of the cumulative throughput and the mean speed.

I. Introduction

With significant advancements in urbanization and motorization, traffic congestion has become a thorny problem in large and medium-sized cities [1]–[5]. In the past decades, researchers have paid much attention to designing efficient management and control strategies for urban transport systems [6]–[11]. Development of efficient signal control strategies for congested networks is one of the most challenging tasks in current research efforts. The challenges consist in the difficulties to establish an exhaustive network traffic flow model, partially because of the lack of valid network traffic demand data, e.g., origin-destination (OD) data, and partially because of the complex nature of travel behaviors [12]. Recently, the macroscopic fundamental diagram (MFD) is considered to be a promising way to model macroscopic network traffic flow using the existing detector data, based on which an effective perimeter control strategy can be contrived to relieve traffic congestion [13], [14]. The main idea of the perimeter control is to regulate traffic flow at the perimeter borders of a protected urban region in order to keep the number of vehicles in the region at a certain critical level.

Since officially introduced in [15], the MFD has become one of the most popular approaches for the macrofeature description of the regional urban network [16]–[19]. It turns out to be an excellent solution to the perimeter control problem of the regional network. The MFD demonstrates a unimodal and low scatter relationship between network vehicle density and network traffic outflow for a homogeneous urban road network, as illustrated in Figure 1. $N(t)$ and $Q(t)$ denote the number of vehicles and the space-mean traffic flow, respectively. N^* represents the critical number of vehicles, at which the maximum space-mean traffic flow Q_m is obtained. When $N(t)$ is less than N^*, the space-mean traffic flow $Q(t)$ increases with the increase of $N(t)$. While $N(t)$ is greater than N^*, the space-mean traffic flow $Q(t)$ decreases with the increase of $N(t)$. When $N(t)$ is near the maximum number of vehicles $N_{\max}$, the space-mean traffic flow $Q(t)$ becomes relatively low, resulting in serious congestion problems. The existence

*Corresponding author

of the MFD is verified using the field data in Yokohama, Japan [20]. Furthermore, the well-defined relationship is proven to be the inherent characteristics of an urban road network, and independent of the OD distribution [21], [22]. Additionally, the MFD can not only efficiently simplify the modeling process of the regional urban network at the macroscopic level, but also well describe the corresponding prime characteristics. Consequently, the MFD has been widely applied to contrive real time perimeter control strategies [23], [24].

To evaluate the proposed methodology, extensive simulation tests are conducted, in which the proposed controller is compared with the existing proportional and integral control strategy.

In general, the MFD-based perimeter control methods can be divided into three main categories: a single region, two urban regions, and multiurban regions. Examples for single region control approaches can be found in [25]–[27]. For instance, a proportional and integral (PI) feedback controller is developed in [25], while in [26] a robust PI controller is designed. Subsequently, two model reference adaptive control (MRAC) based perimeter control algorithms (state feedback and output feedback) are developed for a single aggregated urban region with unknown external disturbances such as model errors in regional accumulation and parameter uncertainties in the MFD [27]. When the quantity of vehicles from all origins to destinations can be measured, state feedback is adopted. When only the output is measured, i.e., only the total quantity of vehicles in all regions is measured, output feedback is employed. In the aforementioned three works, the modeled nonlinear systems are linearized around the point of interest. The only difference is that in [26], [27] the plant's parameter uncertainty is considered in the linearization process. More exactly, the system model matrices of the linearized nonlinear system are respectively denoted by parameter varying elements [26] and unknown elements [27].

Recent advances toward the so-called two urban region perimeter control are reported in the literature [28]–[31]. With the assistance of the MFD, a model predictive control (MPC)-based perimeter control is developed for two urban regions [28]. In [29], a multiscale MPC approach combining the network level perimeter control and the local level signal control is proposed for a road network with one center region and one periphery. It is worth noting that the control approach is firstly designed in the connected vehicle environment. Taking control input constraints and boundary queue length constraints into account, a MFD-based model is formulated for two-region networks with aggregate boundary queue dynamics, based on which Pontryagin maximum principle is used to design an optimal perimeter control pattern maximizing the total throughput of the road network [30]. The control objectives of the road network should vary with different congestion states. To this end, a boundary hybrid control strategy, which consists of the Bang-Bang controller, the PI controller, and an optimal perimeter control algorithm, is proposed according to the corresponding control objective of the congestion state [31]. As for the optimal control algorithm, it takes two objects, i.e., maximizing the throughput of the road network and minimizing the number of blocked vehicles as a whole optimization objective.

During the last years, multiurban region-based control strategies have been extensively studied, see, e.g., [32]–[37]. Based on the linearized model around the equilibrium point, two control strategies, namely multi-variable linear quadratic feedback regulator and linear quadratic integral feedback regulator, are respectively proposed [32]. Within the hierarchical multi-level framework, a control scheme blending the switching timing plan and the perimeter control concept is contrived [33], where the perimeter control problem of the large-scale road network is formulated as a mixed-integer optimization problem. In [34], the original nonlinear dynamics of a bi-modal multi-region road network are approximated by a linear parameter varying model with uncertain parameter at the equilibrium point, and then based on that, a PI controller is proposed to maximize the throughput of the system. With the help of the

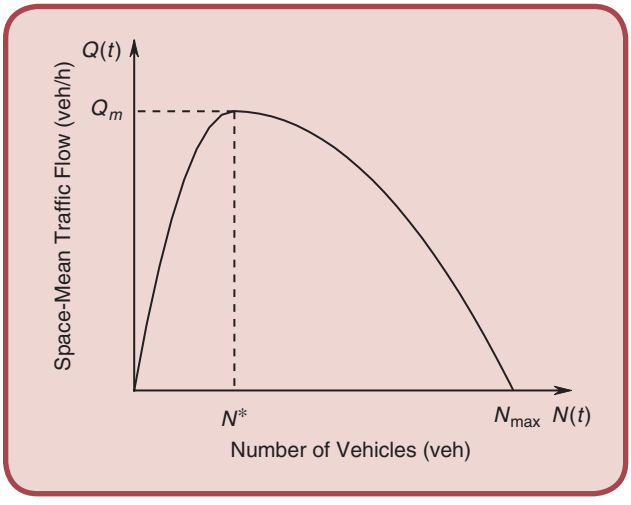

FIG 1 Schematic diagram of the MFD.

piecewise linear approximation concept, the MFDs of the regions are approximated with piecewise affine functions and then a linear MPC-based perimeter control is exploited [35]. Different from the previous works that adopt the centralized approach, a distributed MRAC perimeter control is designed in [36]. More recently, within the MRAC framework, a fully decentralized resilient perimeter control technique is developed to deal with cyberattacks, control input constraints, and uncertainties in the perimeter control problem [37]. Note that in [36] and [37] the original nonlinear systems are linearized around the operation point before designing controllers. In the local region linearization process, to model the plant's parameter uncertainty, the system model matrix is denoted by unknown elements and a certain nonlinear term is introduced to address the higher-order residual in the linearization.

The aforementioned achievements in the perimeter control setting all have been obtained by partially linearizing the system model, which belongs to a local linearization. Actually, the road network system is a nonlinear system and the local linearization probably leads to low traffic performances. Thus, the system's throughput can not be maximized. Hence, this paper aims to design a linearization method for the considered traffic system but in a global linearization setting. Without loss of generality, we focus on the perimeter control for a single urban region. In essence, the designed method can be easily extended to design controllers for multi-region networks. To the best of our knowledge, feedback linearization method is a class of nonlinear control methodologies that can provide a linear model with a precise description of the original nonlinear model among a wide set of the operating points [38], [39]. To this end, based on feedback linearization, this paper proposes a novel perimeter controller for a single urban region. The resulting algorithm is named as the feedback linearization-based PI perimeter controller.

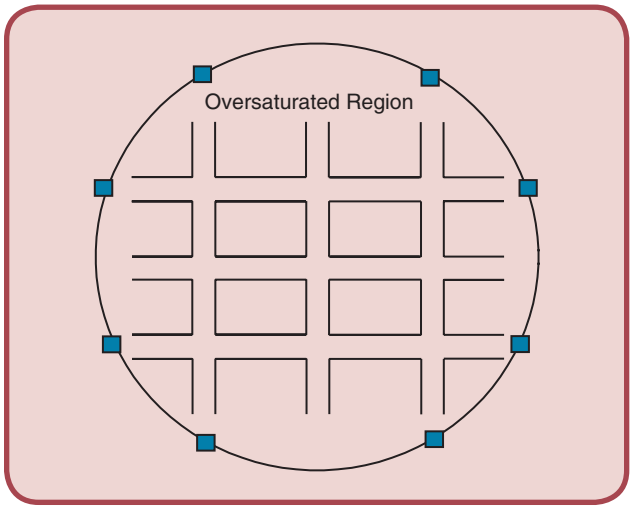

FIG 2 Schematic diagram of the protected network.

Outline: Section II formulates the nonlinear transport system dynamics. The proposed feedback linearization-based PI perimeter controller and its analysis are explained in Section III, while Section IV takes a 5 × 5 homogeneous grid network as an example to validate the effectiveness of the proposed controller. Finally, Section V summarizes the study.

II. System Modeling

Figure 2 shows the morning peak traffic scenario where the majority of travelers are commuting to their workplaces from the outside of the network. The external and internal rectangles represent the periphery of the oversaturated region and internal intersections, respectively. The oversaturated region is the so-called protected network (PN). Following the MFD-based macroscopic traffic network modeling process in [25], the oversaturated region dynamics are presented as follows. In the sequel, it is assumed that the considered region can be described by a well-defined and low-scatter MFD. Then, the conservation equation for vehicles in the considered scenario can be described as

$$\dot{N}(t) = Q_{\text{in}}(t) + Q_d(t) - Q_{\text{out}}(t) \tag{1}$$

where $N(t)$ is the total number of vehicles in the PN at time t; $Q_{\text{in}}(t)$ and $Q_{\text{out}}(t)$ represent the gated inflow entering the PN and the total outflow, respectively; $Q_d(t)$ denotes the nongate controlled or internal inflows to the PN (disturbance). Based on the assumption that there is a proportional relation between the outflow $Q_{\text{out}}(t)$ and the trip completion flow $G[N(t)]$, we have

$$Q_{\text{out}}(t) = \rho G[N(t)] \tag{2}$$

where $G[N(t)]$ is a nonlinear best fitting function of $N(t)$ and $0 < \rho < 1$. Then, substituting (2) into (1), it is immediate to see that

$$\dot{N}(t) = -\rho G[N(t)] + Q_{\text{in}}(t) + Q_d(t). \tag{3}$$

III. Control Design

This section explains whether it is possible to design a controller such that the number of vehicles in the PN is around the critical value N^* in order to maximize the throughput of the PN. Since the dynamics of the PN are nonlinear, input-output feedback linearization can be used to facilitate the control design. Thus, we firstly present a brief description of input-output feedback linearization. Consider the following single-input-single-output nonlinear system:

$$\begin{cases} \dot{x} = f(x) + g(x)u \\ y = h(x) \end{cases} \tag{4}$$

where $x \in \mathbb{R}^n$ is the state vector of the dynamic system; $u \in \mathbb{R}$ represents the control input vector; $y \in \mathbb{R}$ is the system output. $f(\cdot)$, $g(\cdot)$, and $h(\cdot)$ are sufficiently smooth functions in a domain $\mathbb{D} \subset \mathbb{R}^n$. The mappings $f(\cdot) : \mathbb{D} \to \mathbb{R}^n$ and $g(\cdot) : \mathbb{D} \to \mathbb{R}^n$ are so-called vector fields on $\mathbb{D}$. The goal of feedback linearization is to contrive a control law u to obtain a linear input-output map between the new input v and the output y, as shown in Fig. 3.

With the above input-output feedback linearization technique in mind, the following feedback linearization-based controller is well contrived for the considered problem

$$Q_{\text{in}}(t) = \rho G[N(t)] + k_p e(t) + k_i \int_0^t e(t)\,dt \tag{5}$$

where k_p and k_i represent the positive proportional and integral gains, respectively. And

$$e(t) = N^* - N(t). \tag{6}$$

To verify the stability of the system under the proposed controller, the following assumption and lemma are required.

Assumption 1: $Q_d(t)$ is bounded and has a constant value in steady state, that is, $\int_0^\infty \| Q_d(t) \| dt < \infty$; $\lim_{t\to\infty} Q_d(t) = D$, where D is a constant.

Lemma 1: [40] The following single-input linear system

$$\dot{x}(t) = Ax(t) + Bu(t)$$

is asymptotically stable if A is a Hurwitz matrix and u is bounded and satisfies $\lim_{t\to\infty} u(t) = 0$.

By taking the derivate of $e(t)$, we have

$$\dot{e}(t) = -\dot{N}(t). \tag{7}$$

Next, substituting (3) and (5) into (7), the dynamic equation of error e is given by

$$\dot{e}(t) = -k_p e(t) - k_i \int_0^t e(t)\,\mathrm{d}t - Q_d(t). \tag{8}$$

Taking the derivate on both sides of (8), it deduces

$$\ddot{e}(t) + k_p \dot{e}(t) + k_i e(t) = -\dot{Q}_d(t). \tag{9}$$

For the sake of simplicity, let us denote $\Phi(t) = [e(t), \dot{e}(t)]^T$. Then we can write (9) as

$$\dot{\Phi}(t) = C\Phi(t) + D\dot{Q}_d(t) \tag{10}$$

where

$$C = \begin{bmatrix} 0 & 1 \\ -k_i & -k_p \end{bmatrix}, \; D = \begin{bmatrix} 0 \\ -1 \end{bmatrix}.$$

According to Assumption 1 and Lemma 1, it is immediately concluded that $\Phi(t)$ is asymptotically stable, which in turn implies $e(t)$ is asymptotically stable. That is to say, when t tends to ∞, $e(t)$ approaches 0. Now, the proof of the stability is completed.

When taking a more detailed look of the solution to the linear time-invariant differential equation (10), one can have

$$\Phi(t) = \Gamma(t)\Phi(0) + \int_0^t \Gamma(t-\tau) D\dot{Q}_d(\tau)\,d\tau \tag{11}$$

where $\Phi(0)$ is the initial value of the system state; $\Gamma(t) = \exp(Ct)$ and $\Gamma(t-\tau) = \exp[C(t-\tau)]$.

With the above derivation, it is ready to state the following result.

Theorem 1: Consider the nonlinear dynamics given in (3) and the controller in (5). Then the error $e(t)$ converges to zero exponentially under Assumption 1.

Remark 1: As for the value of "ρ", since it is dependent on the urban network. Hence, it can be estimated in advance based on the system parameter identification theory.

Remark 2: In fact, Theorem 1 implies the designed controller can regulate the number of vehicles in the PN to the critical value N^*. Consequently, the throughput of the road network can be maximized.

Remark 3: From (11), it is observed that one can adjust k_p and k_i to achieve a desired exponential convergence rate. Furthermore, the exponential convergence rate guarantees satisfactory transient performances, which is important in practical applications because it can improve the efficiency of the transport system with respect to travel delay, queue length, and mean speed.

Remark 4: It should be pointed out that Theorem 1 is valid only for the case with no input constraints. As known for the constrained nonlinear systems, it is challenging to do a stability analysis in the general case of $\dot{x}(t) = f(x) + sat(u(t))$. Due to technical difficulty, we have not given a rigorous result. One may doubt the availability of the proposed method under the input constraints. To this end, the effectiveness and the stability of the proposed controller for the considered system have been illustrated with numerical simulations as shown in Section IV, where the input constraints $0 \le Q_{\text{in}}(t) \le Q_{\max}$ are considered.

IV. Simulation Results

This section aims to show the effectiveness of the proposed feedback linearization-based PI perimeter controller. To

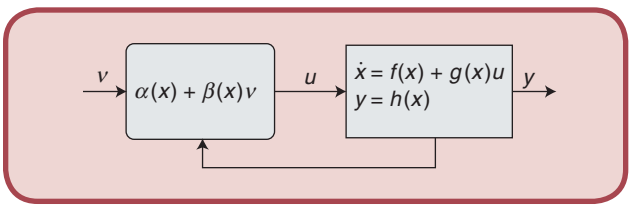

FIG 3 General schematic of feedback linearization.

this end, let us consider a typical morning peak traffic scenario on a homogeneous grid network and its numerical and microsimulation tests are conducted in the following subsections. A comparison with the local linearized control approach proposed in [25] is carried out to show the superiority of our proposed controller.

A. Network Description

A 5 × 5 homogeneous grid network is built in a microscopic traffic simulator Simulation of Urban Mobility (SUMO) [41], as shown in Fig. 4. All internal links have the same length of 250 m. The 20 gating links on the perimeter of the network are 600 m in length to provide sufficient space for the gated vehicles. For the OD distribution of the traffic demand, 80% of the origins will be on the gating links, and 80% of the destinations will be on the internal links. Note that the other 20% traffic demand is the so-called disturbance demand. This could be a case of a typical morning peak scenario where a major part of traffic is traveling to their workplaces in the center of a city. To reflect route choice behaviors of realistic travelers, the routes of vehicles are determined through an iterative assignment process for dynamic user equilibrium. The OD distribution and the route generation are accomplished by the "randomTrip" and "duaIterate" tools provided by SUMO [41]. In addition, to generate a basic operation condition, the signal timings of the intersections are initialized by the Webster method [42]. Then, the MFD can be obtained by fitting the data collected from the simulation (collected every 60 s). In the subsequent simulations, the signal cycle length is 60 s. The total simulation time is three hours, where in the first hour the total traffic demand is set to 3600 veh/h. For the congestion creation, the demand is increased to 9700 veh/h in the second hour, while the demand is again 3600 veh/h in the last hour.

Signal control for the nonperimeter control situation corresponds to the typical fixed-time one. The maximum green time is set to 56 s and the arrival rate for each gate link is assumed to be 2 veh/s. Then the maximum capacity $Q_{\text{in}}^{\max}$ is 560 veh/min. The resulting MFD without applying any perimeter control algorithm is shown in Fig. 5, from which we can observe that N^* is approximately equal to 750 veh and when the number of the vehicle is greater than 750, the road network gradually encounters congestion. The shape of the MFD can be fitted as an exponential function of $N(t)$, e.g., $G[N(t)] = v * t * \exp(-1/a * (t/750)^a) + b$ [37]. By resorting to the least squares fitting method, we get the parameters of the MFD curve as $v = 23.62$, $a = 1.582$, and $b = -629$.

B. Numerical Tests

In this subsection, the numerical simulation is presented to illustrate the transient performance of both controllers. The numerical simulation is conducted with MATLAB. The dynamics of the considered road network are generated via (3). The model parameters are obtained from the traffic scenario simulated in SUMO. Both controllers aim to regulate the number of vehicles in the PN to the set point $N^* = 750$ veh. Two scenarios are simulated to analyze the effect of the proposed feedback linearization-based PI perimeter controller, where the initial accumulation $N(0)$ are 590 veh and 1000 veh, respectively. The parameters of the FLPI method are $k_p = 0.45$ and $k_i = 0.08$, while the parameters of the PI method are $K_p = 0.45$ and $K_i = 0.08$. Thereafter, we denote the no perimeter control, the controller in [25], and our controller as NPC, PI, and FLPI, respectively. As for the PI controller, the original system is linearized around the point $0.9N^*$.

Before showing superiority, we illustrate the stability performance of the FLPI method for the considered system under

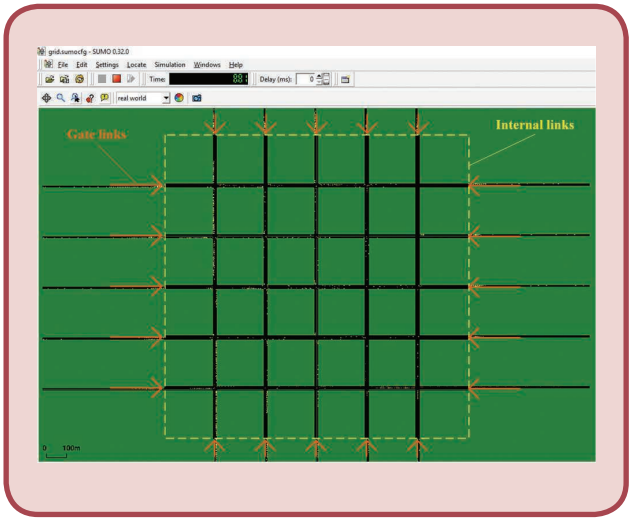

FIG 4 5 × 5 homogeneous grid network used for simulation.

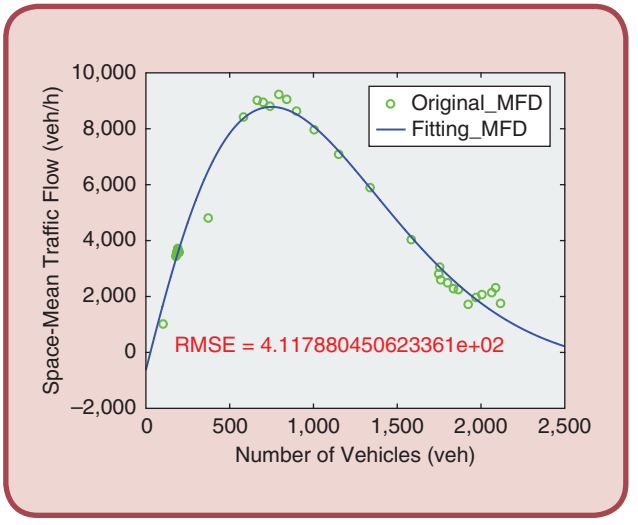

FIG 5 The MFD without any controller.

the input control constraints. As an example, Fig. 6 depicts the stability performance of the FLPI method with a set of various initial accumulation state values $N(0)$ ranging from 500 veh to 1100 veh in steps of 150. To reflect the physical constraints, the input constraints $0 \le Q_{\text{in}}(t) \le Q_{\max}$ are incorporated into the implementation. Accordingly, the control inputs related to all the initial states are presented in Fig. 6(b). The simulation results have validated that the FLPI method can steer all the initial traffic states of practical interest to the desired one under the input constraints.

Furthermore, the behaviors of both controllers are plotted in Figs. 7 and 8, while the perimeter controllers are illustrated in Fig. 9. As expected, both controllers can regulate the traffic state to the desired one. Although both controllers can regulate the traffic state to the desired one, it is obvious that the proposed controller can drive the system state to the set point in a faster manner than that in [25]. In Figs. 7(a) and 8(a), the system state can converge to the set point within 20 control step under the FLPI method, while under the PI method, it takes more. Accordingly under the FLPI method, the maximum throughput of the considered network can be achieved earlier and faster, as shown in Figs. 7(b) and 8(b). Also from Figs. 7 and 8, we can see that the PI method exhibits a larger overshoot than the FLPI method while the FLPI method performs a relatively smooth convergence to its steady state. As a result, the PI method exhibits a lower traffic performance, such as longer travel delay and lower mean speed as presented in the following subsection. It should be highlighted that, although tuning the P and I parameters in the PI method might result in a better performance, the P and I parameters in both controllers are set the same in the simulation while

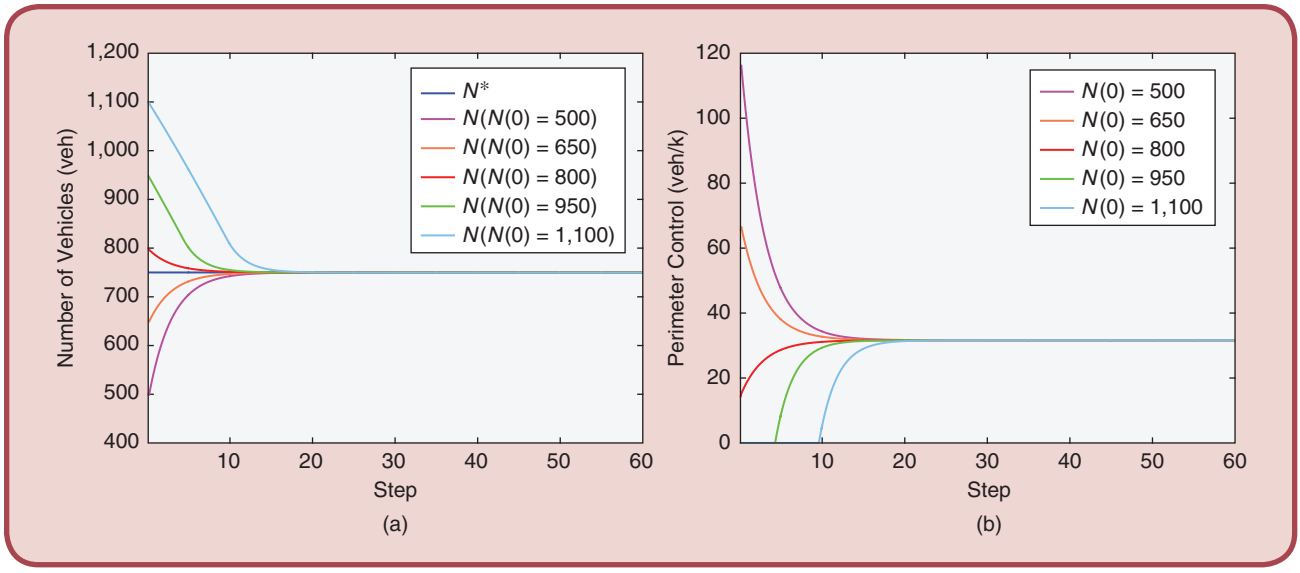

FIG 6 Stability performance. (a) Evolution of accumulations. (b) Perimeter controllers.

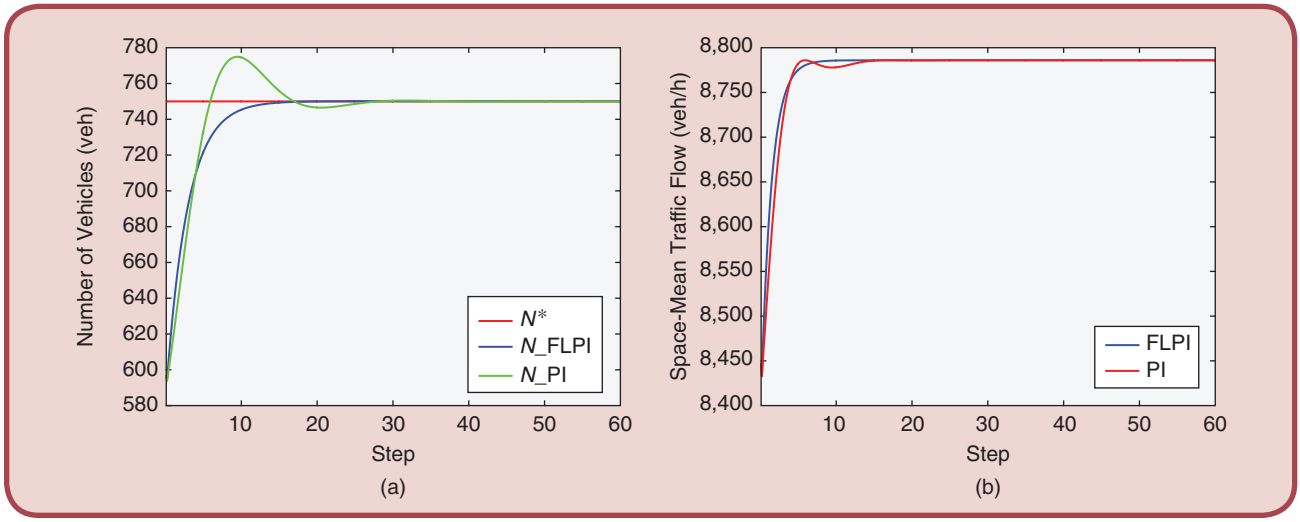

FIG 7 Comparison with the initial accumulation 590 veh. (a) Evolution of accumulations. (b) Throughput of the road network.

the controllers perform differently. The reason behind is that in both scenarios, the system experiences nonlinearity. Furthermore, if the protected network operates in the free flow situation, both controllers might behave the same since under this condition the system is almost linear.

C. Microsimulation Tests

In this subsection, microsimulation tests are presented. The main goal of the tests is to attest the effectiveness of our proposed controller on a more realistic road network and practical traffic scenario. Considering the network will not encounter congestion under the demand 3600 veh/h, the perimeter controller is not triggered in the first hour. The PI and FLPI control algorithms are programmed in simulation and activated every 60 s. The control outputs represent the total traffic demand permitted to enter the network, which is equally assigned to each gating link. To ease the implementation, a signal controller with two-stage timing scheme is used to regulate the entering flow at the end of each gating link. The two-stage timing scheme switches between the green and red lights at a fixed cycle of 60 s. The minimum green time is set to 5 s to allow at least a small portion of vehicles to enter the network during each signal cycle.

For a comprehensive comparison, 10 independent replications for each investigated case (NPC, PI, and FLPI) are performed in the following simulations. The cumulative throughput (CT) and the mean speed (MS) have been computed as performance metrics. The CT is the sum of the throughput over time, while the MS is the speed averaged over time. The results for the three cases are respectively presented in Figs. 10 and 11. As shown in Fig. 11(a), the fixed-time control results in an oversaturated traffic situation, and even in a partial gridlock. From Fig. 10, it is observed that when the PN becomes congested, both the PI method and the

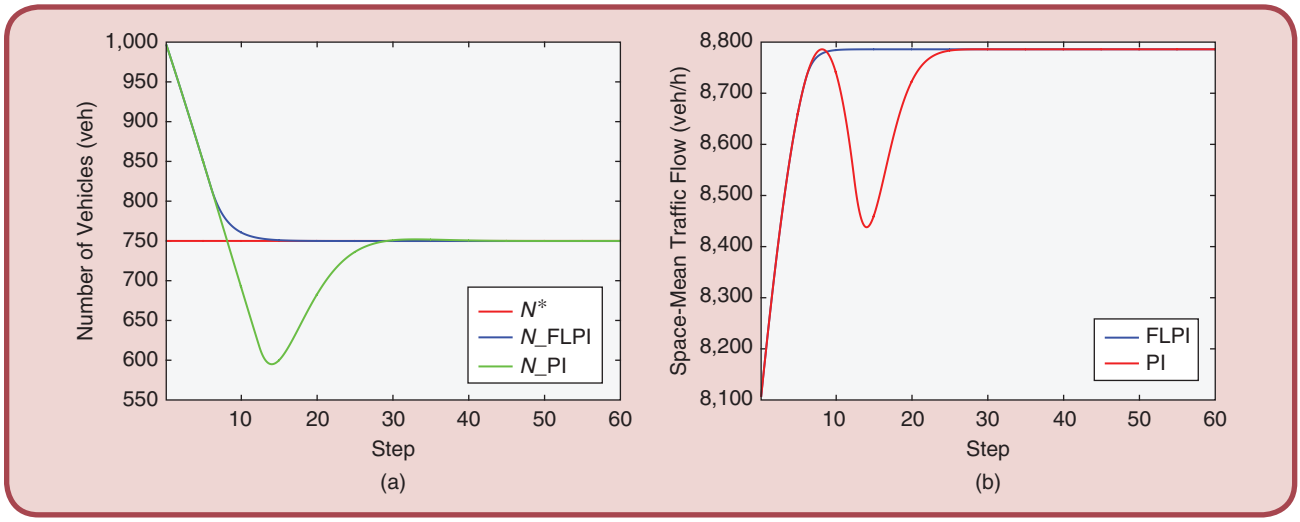

FIG 8 Comparison with the initial accumulation 1000 veh. (a) Evolution of accumulations. (b) Throughput of the road network.

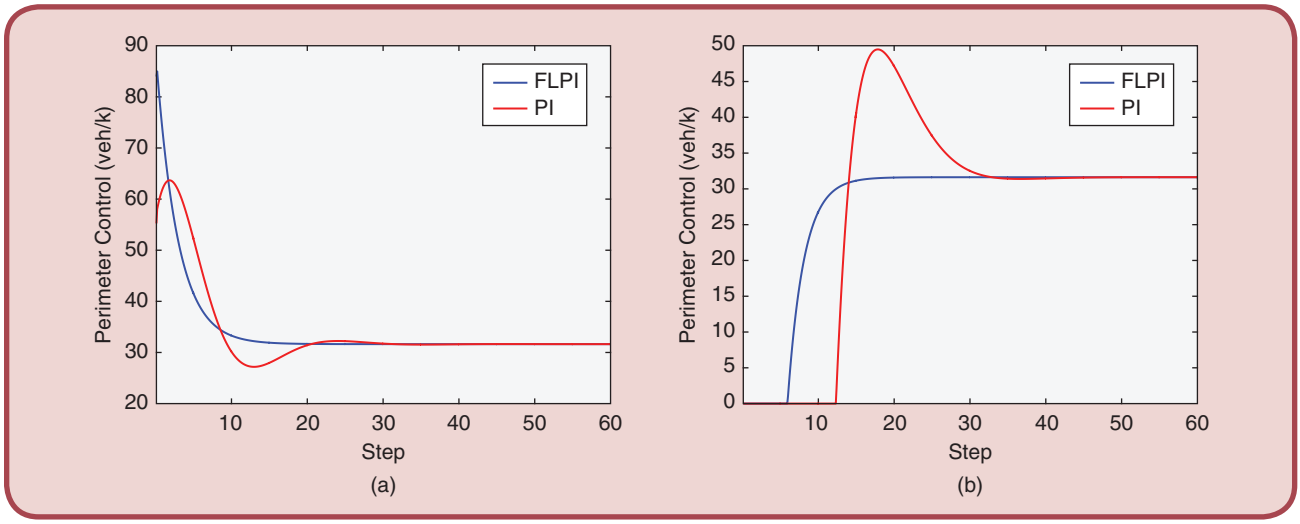

FIG 9 Perimeter controllers. (a) The initial accumulation 590 veh. (b) The initial accumulation 1000 veh.

FLPI method can effectively restrict vehicles at the periphery of the PN to enter the PN. Besides, compared with the PI method, the proposed FLPI method is able to regulate the traffic state to the desirable one faster. Concentrating on Fig. 11(b), although the PI control strategy can avoid the traffic congestion, it does not fully use the network capacity and we can see that the proposed FLPI method can improve the throughput of the road network significantly, which indicates the operational efficiency improvement of the congested network.

Table I compares the CT and the MS. The controller parameters of the two tests are shown in Table II. Obviously, the perimeter controller can enhance the performance of the network. Furthermore, our proposed controller performs better in terms of the CT and the MS than the controller in

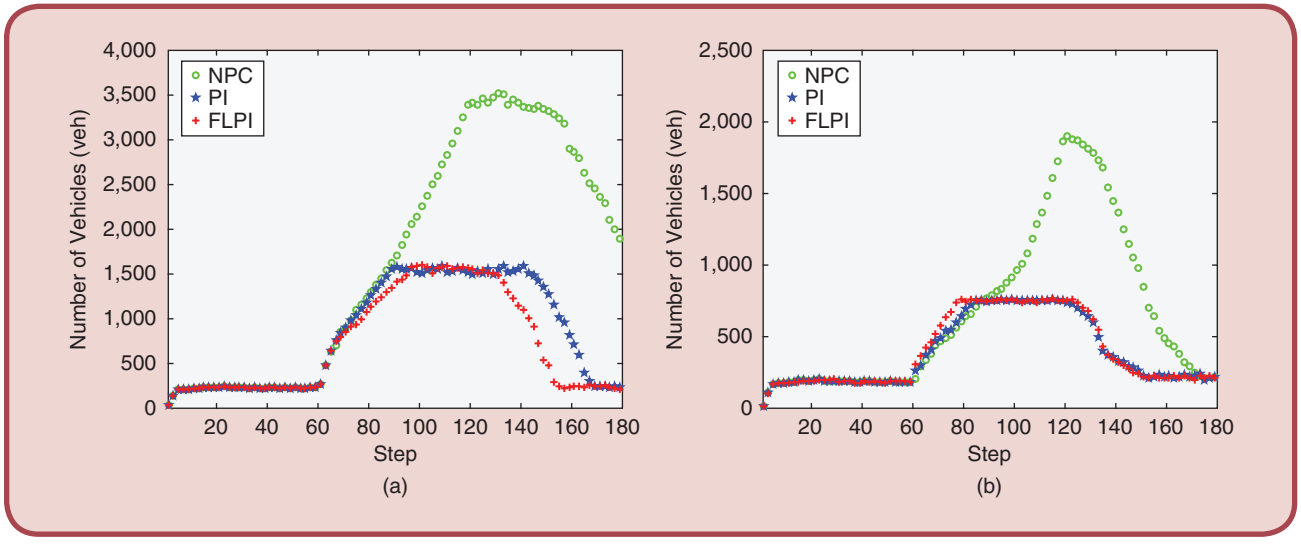

FIG 10 Evolution of accumulations. (a) Vehicles in the network. (b) Vehicles in the protected zone.

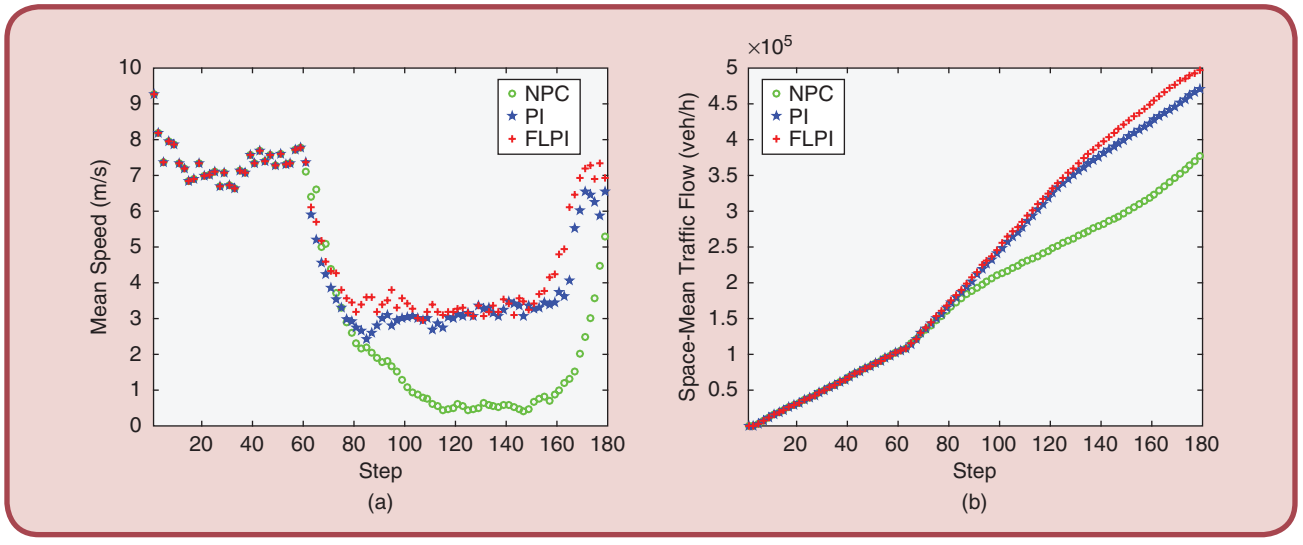

FIG 11 Performance comparison. (a) The mean speed. (b) The cumulative throughput curve.

Table I. Performance comparison in terms of CT and MS.

Control Method	Test 1		Test 2	
	CT (veh.m/s)	MS (m/s)	CT (veh.m/s)	MS (m/s)
NPC	7.6477×10^5	3.8463	7.2380×10^5	3.7041
PI	9.4452×10^5	4.3832	8.6370×10^5	4.0051
FLPI	9.9504×10^5	5.0049	9.4125×10^5	4.6213

Table II. Controller parameters of the PI method and the FLPI method.

Control Method	Test 1		Test 2	
	Proportional Gain	Integral Gain	Proportional Gain	Integral Gain
PI	0.085	0.001	0.12	0.001
FLPI	0.085	0.001	0.12	0.001

[25]. In Test 1, under the FLPI method, when compared with the PI method, the MS is increased by 14.1%. Accordingly, the CT is increased by 5.4%. Similarly, in Test 2, the CT and the MS are respectively increased by 8.9% and 15.4%.

V. Conclusion

This paper has attempted to address the perimeter control problem in a single urban region. Based on the MFD, a feedback linearization-based PI perimeter controller has been successfully applied to alleviate traffic congestion. Different from the existing linearization methods, a global linearization method has been developed, which avoids the underlying divergent system performance. The effectiveness and superiority of the proposed approach has been verified via simulations. Numerical simulations have demonstrated that the proposed FLPI method exhibits a faster and smoother performance than the PI method in [25], while microsimulations have shown that the FLPI method outperforms the PI method in terms of the CT and the MS. Note that the designed method can be easily extended to design controllers for multiregion networks. In the future research we will integrate nonlinear uncertainty suppression and optimality in the control design. In addition, a comprehensive theoretical stability analysis will also be a future research direction, where we will explore other control techniques to take input constraint and uncertainty into consideration.

Acknowledgment

This work was supported by the National Natural Science Foundation of China under Grant 71871055, Grant 61973081, and Grant U1531104, in part by the Key Research and Development Program of Jiangsu under Grant BE2017027, and in part by the Priority Academic Program Development of Jiangsu Higher Education Institutions.

About the Authors

Qian Chen received the M.S. degree in control theory and control engineering and the B.S. degree in automation both from Hohai University, Nanjing, China, in 2014 and 2017, respectively. She is currently pursuing the Ph.D. degree in control science and engineering at Southeast University, Nanjing, China.

Her research interests include intelligent transportation systems, nonlinear control, traffic analysis and control, and nonlinear filtering.

Chengchuan An is currently pursuing the Ph.D. degree at the Intelligent Transportation System Research Center, Southeast University, China. From 2014 to 2016, he was a visiting student at the Department of Civil and Architectural Engineering and Mechanics, University of Arizona, USA.

His current research interests include traffic signal optimization, urban traffic flow modelling, and traffic data mining.

Jingxin Xia is a professor at the Intelligent Transportation System Research Center, Southeast University, China. He received the Ph.D. degree of transportation engineering at the University of Kentucky, USA in 2006.

He has published more than forty peer-reviewed papers so far, and his main research interests include traffic flow theory, transportation network modeling, traffic signal control, and intelligent transportation systems.

Wenming Rao received the B.S. degree in traffic engineering from Northeast Forestry University, Harbin, China, in 2007, and the M.S. degree in traffic engineering from Southeast University, Nanjing, China, in 2012. He is currently a Ph.D. candidate in traffic engineering at Southeast University, Nanjing, China.

His research interests include intelligent transportation systems, network modeling, traffic management and control, and traffic simulation.

Shihua Li (SM'10-F'19) was born in Pingxiang, China, in 1975. He earned his B.Eng., M.Sc. and Ph.D. degrees in control science and engineering from Southeast University, Nanjing, China in 1995, 1998 and 2001, respectively. Since 2001, he has been with the School of Automation, Southeast University, where he is currently a Professor and the Director of the Mechatronic Systems Control Laboratory.

His main research interests lie in modeling, analysis, and nonlinear control theory (nonsmooth control, disturbance rejection control, adaptive control, etc.) with applications to mechatronic systems, intelligent transportation systems and others. He is the author or coauthor of over 200 technical papers and two books in these areas.

Dr. Li is a fellow of IEEE and IET, the Chairman of the IEEE Industrial Electronics Society (IES) Nanjing Chapter. He serves as members of the Technical Committees on System Identification and Adaptive Control, Nonlinear Systems and Control and Variable Structure and Sliding Mode Control of the IEEE CSS and members of the Technical Committees on Electrical Machines, and Motion Control of the IEEE Industrial Electronics Society. He serves as associate editors of IEEE Transactions on Industrial Electronics, International Journal of Robust and Nonlinear Control,

IET Control Theory and Applications, etc. He is one of the Clarivate Analytics (originally Thomson Reuters) Highly Cited Researchers (Engineering) all over the world in 2017, 2018 and 2019.

References

[1] P. Balaji, X. German, and D. Srinivasan, "Urban traffic signal control using reinforcement learning agents," *IET Intell. Transp. Syst.*, vol. 4, no. 3, pp. 177–188, Sept. 2010. doi: 10.1049/iet-its.2009.0096.

[2] S. Lin, B. De Schutter, Y. Xi, and H. Hellendoorn, "Efficient network-wide model-based predictive control for urban traffic networks," *Transp. Res. C, Emerg. Technol.*, vol. 24, pp. 122–140, Oct. 2012. doi: 10.1016/j.trc.2012.02.003.

[3] Y. Zhao, H. Gao, S. Wang, and F.-Y. Wang, "A novel approach for traffic signal control: A recommendation perspective," *IEEE Intell. Transp. Syst. Mag.*, vol. 9, no. 3, pp. 127–135, July 2017. doi: 10.1109/MITS.2017.2709779.

[4] P. Kachroo, S. Gupta, S. Agarwal, and K. Ozbay, "Optimal control for congestion pricing: Theory, simulation, and evaluation," *IEEE Trans. Intell. Transp. Syst.*, vol. 18, no. 5, pp. 1234–1240, May 2017. doi: 10.1109/TITS.2016.2601245.

[5] L. A. Garcia and V. R. Tomas, "A smart peri-urban I2V architecture for dynamic rerouting," *IEEE Intell. Transp. Syst. Mag.*, vol. 10, no. 2, pp. 69–79, Apr. 2018. doi: 10.1109/MITS.2018.2806635.

[6] E. B. Kosmatopoulos, M. Papageorgiou, A. Vakouli, and A. Kouvelas, "Adaptive fine-tuning of nonlinear control systems with application to the urban traffic control strategy TUC," *IEEE Trans. Control Syst. Technol.*, vol. 15, no. 6, pp. 991–1002, Nov. 2007. doi: 10.1109/TCST.2007.899645.

[7] K. Han, H. Liu, V. V. Gayah, T. L. Friesz, and T. Yao, "A robust optimization approach for dynamic traffic signal control with emission considerations," *Transp. Res. C, Emerg. Technol.*, vol. 70, pp. 3–26, Sept. 2016. doi: 10.1016/j.trc.2015.04.001.

[8] F. Yan, F. Tian, and Z. Shi, "Iterative learning approach for traffic signal control of urban road networks," *IET Control Theory Appl.*, vol. 11, no. 4, pp. 466–475, Feb. 2017. doi: 10.1049/iet-cta.2016.0376.

[9] I. I. Sirmatel and N. Geroliminis, "Mixed logical dynamical modeling and hybrid model predictive control of public transport operations," *Transp. Res. B, Methodol.*, vol. 114, pp. 325–345, Aug. 2018. doi: 10.1016/j.trb.2018.06.009.

[10] I. Kalamaras et al., "An interactive visual analytics platform for smart intelligent transportation systems management," *IEEE Trans. Intell. Transp. Syst.*, vol. 19, no. 2, pp. 487–496, Feb. 2018. doi: 10.1109/TITS.2017.2727143.

[11] A. Aboudina, I. Kamel, M. Elshenawy, H. Abdelgawad, and B. Abdulhai, "Harnessing the power of HPC in simulation and optimization of large transportation networks: Spatio-temporal traffic management in the greater Toronto area," *IEEE Intell. Transp. Syst. Mag.*, vol. 10, no. 1, pp. 95–106, Jan. 2018. doi: 10.1109/MITS.2017.2776123.

[12] H. Fu, N. Liu, and G. Hu, "Hierarchical perimeter control with guaranteed stability for dynamically coupled heterogeneous urban traffic," *Transp. Res. C, Emerg. Technol.*, vol. 83, pp. 18–38, Oct. 2017. doi: 10.1016/j.trc.2017.07.007.

[13] M. Keyvan-Ekbatani, M. Yildirimoglu, N. Geroliminis, and M. Papageorgiou, "Multiple concentric gating traffic control in large-scale urban networks," *IEEE Trans. Intell. Transp. Syst.*, vol. 16, no. 4, pp. 2141–2154, Aug. 2015. doi: 10.1109/TITS.2015.2399303.

[14] I. I. Sirmatel and N. Geroliminis, "Economic model predictive control of large-scale urban road networks via perimeter control and regional route guidance," *IEEE Trans. Intell. Transp. Syst.*, vol. 19, no. 4, pp. 1112–1121, Apr. 2018. doi: 10.1109/TITS.2017.2716541.

[15] C. F. Daganzo, "Urban gridlock: Macroscopic modeling and mitigation approaches," *Transp. Res. B, Methodol.*, vol. 41, no. 1, pp. 49–62, Jan. 2007. doi: 10.1016/j.trb.2006.03.001.

[16] V. V. Gayah, X. S. Gao, and A. S. Nagle, "On the impacts of locally adaptive signal control on urban network stability and the macroscopic fundamental diagram," *Transp. Res. B, Methodol.*, vol. 70, pp. 255–268, Dec. 2014. doi: 10.1016/j.trb.2014.09.010

[17] M. Ramezani, J. Haddad, and N. Geroliminis, "Dynamics of heterogeneity in urban networks: Aggregated traffic modeling and hierarchical control," *Transp. Res. B, Methodol.*, vol. 74, pp. 1–19, Apr. 2015. doi: 10.1016/j.trb.2014.12.010.

[18] F. Yan, F. Tian, and Z. Shi, "An extended signal control strategy for urban network traffic flow," *Phys. A, Stat. Mech. Appl.*, vol. 445, pp. 117–127, Mar. 2016. doi: 10.1016/j.physa.2015.10.047.

[19] K. An, Y.-C. Chiu, X. Hu, and X. Chen, "A network partitioning algorithmic approach for macroscopic fundamental diagram-based hierarchical traffic network management," *IEEE Trans. Intell. Transp. Syst.*, vol. 19, no. 4, pp. 1130–1139, July 2018. doi: 10.1109/TITS.2017.2713808.

[20] N. Geroliminis and C. F. Daganzo, "Existence of urban-scale macroscopic fundamental diagrams: Some experimental findings," *Transp. Res. B, Methodol.*, vol. 42, no. 9, pp. 759–770, Nov. 2008. doi: 10.1016/j.trb.2008.02.002.

[21] N. Geroliminis and J. Sun, "Properties of a well-defined macroscopic fundamental diagram for urban traffic," *Transp. Res. B, Methodol.*, vol. 45, no. 3, pp. 605–617, Mar. 2011. doi: 10.1016/j.trb.2010.11.004.

[22] V. V. Gayah and C. F. Daganzo, "Clockwise hysteresis loops in the macroscopic fundamental diagram: An effect of network instability," *Transp. Res. B, Methodol.*, vol. 45, no. 4, pp. 643–655, May 2011. doi: 10.1016/j.trb.2010.11.006.

[23] Z. Zhou, B. De Schutter, S. Lin, and Y. Xi, "Two-level hierarchical model-based predictive control for large-scale urban traffic networks," *IEEE Trans. Control Syst. Technol.*, vol. 25, no. 2, pp. 496–508, Mar. 2017. doi: 10.1109/TCST.2016.2572169.

[24] L. Ambühl, A. Loder, M. C. Bliemer, M. Menendez, and K. W. Axhausen, "A functional form with a physical meaning for the macroscopic fundamental diagram," *Transp. Res. B, Methodol*, Nov. 2018. doi: 10.1016/j.trb.2018.10.013.

[25] M. Keyvan-Ekbatani, A. Kouvelas, I. Papamichail, and M. Papageorgiou, "Exploiting the fundamental diagram of urban networks for feedback-based gating," *Transp. Res. B, Methodol.*, vol. 46, no. 10, pp. 1393–1403, Dec. 2012. doi: 10.1016/j.trb.2012.06.008.

[26] J. Haddad and A. Shraiber, "Robust perimeter control design for an urban region," *Transp. Res. B, Methodol.*, vol. 68, pp. 315–332, Oct. 2014. doi: 10.1016/j.trb.2014.06.010.

[27] J. Haddad and B. Mirkin, "Adaptive perimeter traffic control of urban road networks based on MFD model with time delays," *Int. J. Robust Nonlinear Control*, vol. 26, no. 6, pp. 1267–1285, Jan. 2016. doi: 10.1002/rnc.3502.

[28] N. Geroliminis, J. Haddad, and M. Ramezani, "Optimal perimeter control for two urban regions with macroscopic fundamental diagrams: A model predictive approach," *IEEE Trans. Intell. Transp. Syst.*, vol. 14, no. 1, pp. 348–359, Mar. 2013. doi: 10.1109/TITS.2012.2216877.

[29] K. Yang, N. Zheng, and M. Menendez, "Multi-scale perimeter control approach in a connected-vehicle environment," *Transp. Res. C, Emerg. Technol.*, vol. 94, pp. 32–49, Sept. 2018. doi: 10.1016/j.trc.2017.08.014.

[30] J. Haddad, "Optimal perimeter control synthesis for two urban regions with aggregate boundary queue dynamics," *Transp. Res. B, Methodol.*, vol. 96, pp. 1–25, Feb. 2017. doi: 10.1016/j.trb.2016.10.016.

[31] H. Ding, Y. Zhang, X. Zheng, H. Yuan, and W. Zhang, "Hybrid perimeter control for two-region urban cities with different states," *IEEE Trans. Control Syst. Technol.*, vol. 26, no. 6, pp. 2049–2062, Nov. 2018. doi: 10.1109/TCST.2017.2746061.

[32] K. Aboudolas and N. Geroliminis, "Perimeter and boundary flow control in multi-reservoir heterogeneous networks," *Transp. Res. B, Methodol.*, vol. 55, pp. 265–281, Sept. 2013. doi: 10.1016/j.trb.2013.07.003.

[33] M. Hajiahmadi, J. Haddad, B. D. Schutter, and N. Geroliminis, "Optimal hybrid perimeter and switching plans control for urban traffic networks," *IEEE Trans. Control Syst. Technol.*, vol. 23, no. 2, pp. 464–478, Mar. 2015. doi: 10.1109/TCST.2014.2330997.

[34] K. Ampountolas, N. Zheng, and N. Geroliminis, "Macroscopic modelling and robust control of bi-modal multi-region urban road networks," *Transp. Res. B, Methodol.*, vol. 104, pp. 616–637, Oct. 2017. doi: 10.1016/j.trb.2017.05.007.

[35] A. Kouvelas, M. Saeedmanesh, and N. Geroliminis, "A linear formulation for model predictive perimeter traffic control in cities," *IFAC-PapersOnLine*, vol. 50, no. 1, pp. 8543–8548, July 2017. doi: 10.1016/j.ifacol.2017.08.1411.

[36] J. Haddad and B. Mirkin, "Coordinated distributed adaptive perimeter control for large-scale urban road networks," *Transp. Res. C, Emerg. Technol.*, vol. 77, pp. 495–515, Apr. 2017. doi: 10.1016/j.trc.2016.12.002.

[37] J. Haddad and B. Mirkin, "Resilient perimeter control of macroscopic fundamental diagram networks under cyberattacks," *Transp. Res. B, Methodol.*, Mar. 2019. doi: 10.1016/j.trb.2019.01.020.

[38] R. Marino and P. Tomei, "Dynamic output feedback linearization and global stabilization," *Syst. Control Lett.*, vol. 17, no. 2, pp. 115–121, Aug. 1991. doi: 10.1016/0167-6911(91)90036-E.

[39] G. Oriolo, A. D. Luca, and M. Vendittelli, "WMR control via dynamic feedback linearization: Design, implementation, and experimental validation," *IEEE Trans. Control Syst. Technol.*, vol. 10, no. 6, pp. 835–852, Nov. 2002. doi: 10.1109/TCST.2002.804116.

[40] S. Li, J. Yang, W.-H. Chen, and X. Chen, "Generalized extended state observer based control for systems with mismatched uncertainties," *IEEE Trans. Ind. Electron.*, vol. 59, no. 12, pp. 4792–4802, Dec. 2012. doi: 10.1109/TIE.2011.2182011.

[41] P. A. Lopez et al., "Microscopic traffic simulation using SUMO," in *Proc. 21st IEEE Int. Conf. Intelligent Transportation Systems (ITSC)*, Maui, Nov. 2018, pp. 2575–2582.

[42] F. V. Webster, "Traffic signal settings," Road Research Lab., London, Tech. Rep., 1958.

ITS